Title
A newly calibrated laser-induced fluorescence (LIF) system for Ar ions with a single tunable diode laser

Journal
JOURNAL OF THE KOREAN PHYSICAL SOCIETY, 48(2)

ISSN
0374-4884

Authors
Woo, HJ
Chung, KS
Lho, T
et al.

Publication Date
2006

Journal of the Korean Physical Society, Vol. 48, No. 2, February 2006, pp. 260∼265

A Newly Calibrated Laser-Induced Fluorescence (LIF) System for Ar Ions with a Single Tunable Diode Laser

Hyun-Jong Woo and Kyu-Sun Chung*
electric Probe Applications Laboratory, Hanyang University, Seoul 133-791

Taihyeop Lho
National Fusion Research Center, Korea Basic Science Institute, Daejeon 305-333

Roger McWilliams
Department of Physics and Astronomy, University of California, Irvine, CA 92697, USA

(Received 13 October 2005)

Accurate measurements of the ion velocity distribution function (IVDF), the ion temperature, and the ion drift velocity by laser-induced fluorescence (LIF) are only possible if the accurate laser wavelength during the wavelength scan is known, yet an absolute calibration is not easily achievable because of the non-linear characteristics of the piezo-electric actuator in a diode laser, the small mode-hop free tuning region, and uncertainty of the wavemeter. The LIF system for the Diversified Plasma Simulator (DiPS), which is a simulator for the divertor and space plasmas, is calibrated both by absolute calibration of the wavemeter and by launching diode lasers in opposite directions. In addition, the first result on the measurement of the ion temperature and the flow velocity is given.

PACS numbers: 52.25.Xz, 52.70.Kz, 52.75.Xx
Keywords: Laser-induced fluorescence, LIF, Diode laser, Iodine cell, Ion temperature, Plasma flow velocity

I. INTRODUCTION

After the laser-induced fluorescence (LIF) technique had been introduced for the measurement of the Ar ion velocity distribution function (IVDF) by Stern and Johnson, III in 1975 [1], it has been used for various plasmas to measure the ion flow velocity [2–4], the ion temperature [5, 6], the magnetic field strength [7] and the ion density [8]. For Ar ion diagnostics, the doublet transition is generally used to pump $3d^2G_{9/2}$ metastable ions to the $4p^2F_{7/2}$ excited state by using a single-mode, tunable, high-power dye laser system with a wavelength of 611.66 nm (in vacuum) and the fluorescence signals are measured at 461.08 nm ($4p^2F_{7/2} \rightarrow 4s^2D_{5/2}$) [2, 5, 9]. Severn *et al.* first proposed the diode laser based LIF scheme for Ar ions with a wavelength of 668.61 nm (in vacuum) ($3d^4F_{7/2} \rightarrow 4p^4D_{5/2}$) and measured the fluorescence signals with a wavelength of 442.72 nm ($4p^4D_{5/2} \rightarrow 4s^4P_{3/2}$) [10]. For this LIF scheme, they used two diode lasers: one was a low-power tunable seed laser (<5 mW) with a Littman cavity geometry and the other was a the master oscillator power amplifier (MOPA: <500 mW) with a Littman/Metcalf geometry.

Boivin and Scime also suggested a diode laser based LIF scheme with a single, low-power, tunable diode laser with a Littrow external cavity geometry [11]. Generally, diode lasers with Littrow cavity geometries (<20 mW) produce more output power than diode lasers with Littman cavity geometries (<5 mW), but the former's mode-hop free tuning region (<20 GHz) is typically four times smaller than that of the Littman cavity diode laser (<80 GHz) in the range of wavelengths of 665 – 675 nm [11]. Although some MOPA systems are currently available for this LIF scheme, their mode-hop free tuning region, typically less than 20 GHz, does not cover the region of a low-power seed laser with a Littman cavity geometry. Hence, Boivin and Scime's scheme is considered as an economic and simple LIF system with a diode laser.

The piezo-electric actuator, which is used for the wavelength scan in a diode laser, has non-linear characteristics although it seems to show the linear characteristics [12]. To avoid this non-linearity, one needs to monitor the laser wavelength on-line and that is why the iodine cell spectrum is a powerful method for wavelength monitoring using a diode laser. However, the reference peaks of the iodine cell may be hard to measure with commercially available iodine cell because of the low power of

*E-mail: kschung@hanyang.ac.kr; Fax: +82-2-2299-1908

the diode laser and the weak absorption line of iodine cell. In addition, reference wavelengths, ±20 GHz from the LIF pump transition, do not appear in the standard reference table of iodine peaks [13]. Recently, Keesee *et al.* increased the iodine vapor pressure by heating the iodine cell and measured the wavelengths of the iodine peaks by using a wavemeter [14]. However, we found that their reference wavelengths for the iodine peaks seemed to be shifted by 0.002 nm, which was observed by injecting lasers in the forward and the backward directions during the LIF measurement. This shift of the iodine peak wavelength could conceivably cause an error in deducing the ion flow velocity of 900 m/s.

In this work, the iodine peak wavelengths for the LIF were newly calibrated in stationary plasma both by using absolute calibrations of the wavemeter and by measuring the LIF signals by injecting lasers in the forward and the backward directions. In addition, the iodine flow, possibly caused by local heating of the iodine cell, was checked by rotating the iodine cell heating assembly by 180°, and turned out to be negligible. The LIF system of Diversified Plasma Simulator (DiPS) and its characteristics are introduced for measuring the Ar IVDF, ion temperature, and ion flow velocity with a single, low-power, tunable diode laser.

II. EXPERIMENTAL SET-UP

Experiments were performed in a LaB_6 dc plasma source, which is one of two plasma sources of the DiPS [15]. The LaB_6 in the DiPS is a disk-type with a diameter of 101.6 mm (4 in) and a thickness of 6.35 mm (0.25 in), and it is directly heated by using a graphite heater with a power of up to 4 kW for an Ar plasma and 6 kW for a He plasma. Through high differential pumping with a smaller diameter anode, 20 mm, the pressure of the source region becomes higher than that in the divertor simulation region. Typically, the pressure of source region is 50 – 300 mTorr, and that of the divertor simulation region is 0.1 – 10 mTorr. The electromagnet assembly produces a steady state axial magnetic field strength of up to 2 kG. The typical electron temperature and density are 2 – 3 eV and up to 10^{14} cm^{-3} for an Ar plasma and 5 – 10 eV and up to 10^{13} cm^{-3} for a He plasma. The followings are typical conditions for a current experiment: magnetic field = 430 G, source region pressure = 130 mTorr, divertor simulation region pressure = 2.2 mTorr, electron temperature = 2.5 eV, and electron density = 5 $\times 10^{12}$ cm^{-3}.

Fig. 1 shows a schematic diagram of the LIF system. Currently available diode lasers with Littrow external cavity geometries for an Ar ion LIF have typical output powers of 20 mW and mode-hop free tuning regions of 10 GHz. In this experiment, the TEC-100 model from Sacher Lasertechnik [16] was used with the following specifications: maximum output power = 25 mW at

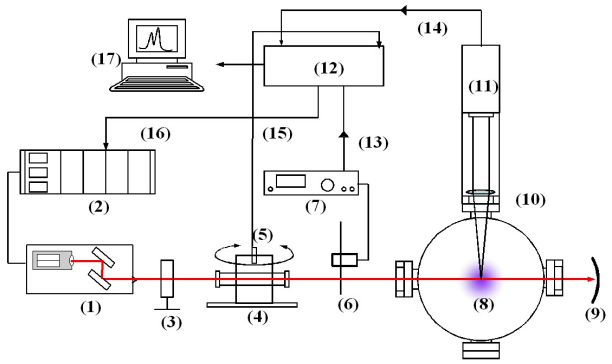

Fig. 1. (Color online) Schematic diagram of the LIF system for DiPS: (1) Littrow external cavity diode laser, (2) laser controller, (3) iris, (4) iodine reference cell, (5) NTE3032 photo-transistor, (6) chopper, (7) chopper controller, (8) plasma, (9) beam dump, (10) imaging lens, (11) PMT tube, (12) lock-in amplifier, (13) reference signal input, (14) fluorescence signal input, (15) iodine cell signal input, (16) voltage ramp, and (17) PC.

668.61 nm (at a −85 mA laser current), line width = 1 MHz, coarse tuning range = 665 – 675 nm with a rotating grating, fine tuning range = 0.34 nm with piezo-electric actuator control from 0 to 100 Volt, and a mode-hop free tuning region≥ 16 GHz, with current coupling method [16]. We prevent the back scatter of the laser beam toward the diode laser by tilting the iodine cell less than 5°, and using the anti-reflection (AR) coated windows [17] in all laser paths without an optical isolator to save the laser power. The iris is also located close to the diode laser to reduce the probability of back scatter of the laser beam back toward the laser. To measure a clear iodine spectrum, we use a commercially available silicon rubber heater to heat the iodine cell as done by Keesee *et al* [14, 18]. The iodine cell in a thick aluminum housing, which is coated with black paint, is heated up to 90 ± 4 °C. A 4 kHz mechanical chopper and the Stanford Research SR830 [19] lock-in amplifier are used to collect only the fluorescence signal by eliminating the electron-impact-induced radiation and the electronic noise. The SR830 lock-in amplifier is also used to measure the iodine cell spectrum with a NTE3032 photo-transistor [20] through its auxiliary input and to ramp the input voltage of the piezo-electric actuator through its auxiliary output with a minimum resolution of 1 mV. The ramp voltage supplied to the laser is amplified by 10 times at the laser controller. The fluorescence signals are collected by the photomultiplier tube (PMT) and filtered by 1 nm bandwidth filter [21] with a center wavelength of 442 nm after having been focused by an imaging lens with a 170 mm focal length.

For diode laser tuning and iodine peak wavelength calibration, the wavemeter of Burleigh (WA-1000) was used [22]. The absolute accuracy and the display resolution of the wavemeter is quoted by Burleigh at +− 0.001 nm. The wavelengths of the iodine peaks were calibrated by

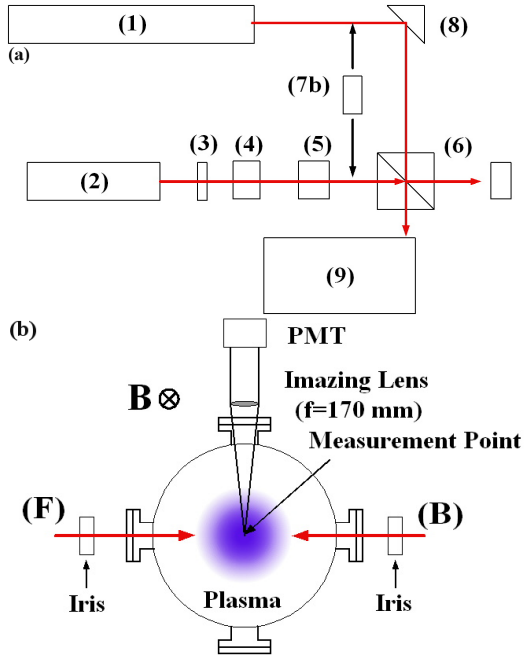

Fig. 2. (Color online) Schematic diagram for the iodine cell calibration: (a) absolute calibration of wavemeter and measurement of the wavelengths of the iodine peaks and (b) calibration of the wavelength shift. For (a), (1) He-Ne laser, (2) TEC100 diode laser, (3) iris, (4) iodine cell, (5) optical isolator, (6) beam splitter, (7) beam dump, (8) mirror, and (9) WA-1000 wave-meter. For (b), (F) and (B) mean the forward and the backward injection of the laser, respectively.

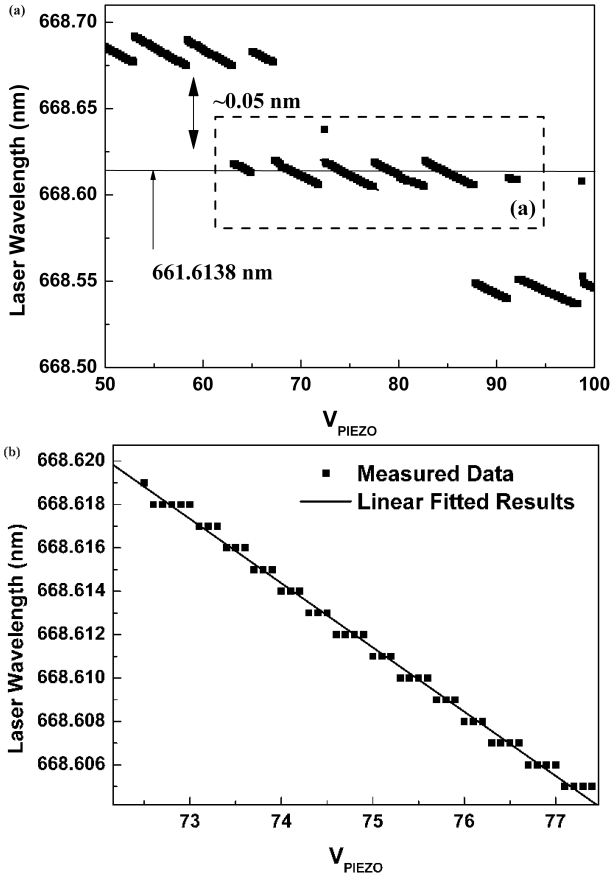

Fig. 3. Characteristics of the diode laser: (a) many mode-hops and repetitions of the same wavelength while the piezo-electric actuator voltage, and (b) the linear characteristics of the mode-hop free tuning region.

using the two schemes: one was an absolute calibration (or checking the statistical uncertainty) of the wavemeter and the other was injection of the lasers in opposite directions during the LIF measurement. These calibration schemes are shown in Fig. 2. In Fig. 2(a), a He-Ne laser, 1125P model from JDS Uniphase [23], was used with a fixed wavelength of 632.8 nm (632.991 nm in vacuum) for the absolute calibration of the wavemeter. The optical isolator, Fig. 2(a), is used to block the 1 mW reference laser from the wavemeter. The beam dump is located in the path of the He-Ne laser while scanning the diode laser in the mode-hop free tuning region and moves in the diode laser path for the wavemeter calibration during mode hop. Except for the collection of LIF signal from the plasma, all the procedures shown in Fig. 2(a) are the same in the case of the LIF measurement. In addition, to check for possible iodine flow in the cell caused by local heating, the input and output sides of the cell were reversed by rotating the cell by 180 degrees. Although the statistical uncertainty of the wavemeter was observed to be ± 0.017 nm at its start-up, there was no problem in generating the accurate wavelengths for the iodine peaks because of the statistical errors of the wavemeter were monitored twice by He-Ne laser, once at the initial step and once at the final step of the mode-hop free scanning of the diode laser. For more accurate calibration of the wavelengths of the iodine peaks, opposite injection of the diode laser, as shown in Fig. 2(b), was performed to check the shifts in the iodine peaks from the displayed wavelengths to other wavelengths because of the display resolution being as large as 0.001 nm. Using irises in both directions of the laser path, one prevents the errors caused by slight changes in the measurement position. The measurement was performed 11 times for the wavemeter depicted in Fig. 2(a) and 10 times in each direction of the laser in Fig. 2(b).

III. RESULTS AND DISCUSSION

The characteristics of the TEC-100 diode laser are shown in Fig. 3. Many mode-hops are seen for piezo-electric actuator voltages from 50 to 100 V (or in fine tuning range of 0.34 nm when the piezo-electric actuator voltage is changed from 0 to 100 V). From Fig. 3(a), mode-hop free tuning regions with almost the same wavelengths are repeated at least four times. Fig. 3(b) shows the laser wavelength, which has almost linear character-

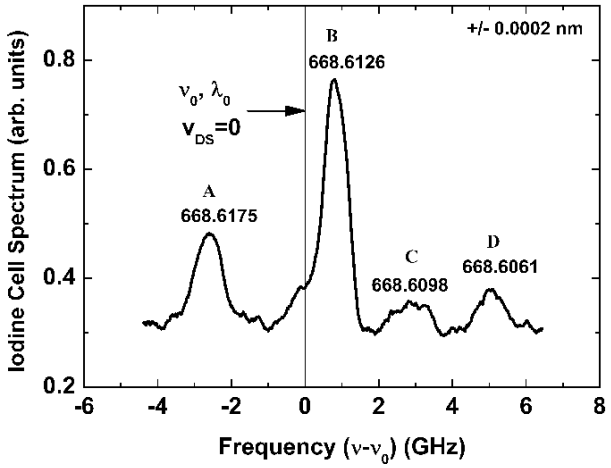

Fig. 4. Newly calibrated iodine cell spectrum vs. frequency shift near the Ar ion LIF scheme. This result differ from the previous results by 0.002 nm (Keesee *et al.*: A = 668.6196 nm, B = 668.6144, C = 668.6119, and D = 668.6079nm with errors of ± 4 pm). ν_0 and λ_0 are the frequency, wavelength at the Ar ion pump transition, which means no Doppler shift (or no plasma drift, $v_{DS} = 0$). ($\nu_0 = 4.4837 \times 10^2$ THz, λ_0 = 668.6138 nm)

istics, measured within the mode-hop free tuning region. The step-like function in the measured data is caused by a limitation of display resolution (0.001 nm). Although the mode-hop free tuning region is reported by the manufacturer to be over 16 GHz for the current coupling method, the measured one was typically 10 GHz. The temperature around the diode laser plays an important role in the variation of the laser wavelength. The difference of the temperatures between winter (−5 °C) and summer (35 °C) in Seoul, South Korea, is about 40 °C and may change the temperature around diode laser by at least 20 °C. In our case, this change shifted the laser wavelength by about 0.2 nm. This is a big shift when comparing the mode-hop free tuning region and the fine tuning region. For stable laser operation, it is important to keep the temperature around the diode laser as constant as possible.

Fig. 4 shows the newly calibrated wavelengths of the iodine peaks for the LIF scheme. The central frequency, $\nu_0 = 4.4837 \times 10^2$ THz, stands for the Ar ion pump transition with a wavelength of 668.6138 nm (in vacuum), as indicated by the black line. These wavelengths were obtained by using two procedures. First, each iodine reference peak's wavelength was measured for a linear fitting range of ±0.03 nm from each peak during a 1 mV voltage ramp on the piezo-electric actuator. The reference peaks' wavelengths, which are shown in Fig. 4, were deduced by averaging eleven sets of measured data. Next, the peak wavelengths were shifted linearly by the LIF measurement, Fig. 2(b), to overcome the display resolution of the wavemeter. Since the LIF measurement is based on the Doppler effect, there is a difference between the two LIF peaks in flowing plasma, but there should be no difference in a stationary plasma when one injects the same laser in opposite directions (bi-directional laser injection), *i.e.* forward and backward. The Ar ion pump transition should be deduced from the central point of the differences between these two LIF peaks. Hence, the wavelengths of the iodine reference peaks measured by the wavemeter were linearly shifted by 0.05 pm. The present results shift in the wavelength, 0.05 pm, was lower than the display resolution of the wavemeter, 1 pm, and the error caused by the linear fitting, ±0.2 pm. These newly calibrated wavelengths of the iodine peaks are different from the previous results by 0.002 nm (Keesee *et al.*: A = 668.6196 nm, B = 668.6144 nm, C = 668.6119 nm, D = 668.6079 nm with errors of ±0.0004 nm) [14], which is the key finding of this paper. This agrees well with the *I2 B-X* spectrum calculated by using the Dunham coefficient given by Gerstenkorn and Luc [24,25]. The iodine atom flow is thought to be possibly caused by local heating of the iodine cell. It should be possible to reduce the errors by an injecting laser into the iodine cell reversely and comparing it with that of forward direction with respect to LIF measurement (or the iodine peak shift to the LIF signal with reverse injection of lasers under the same plasma conditions). Hence, it is very important to make sure that no flow exists in the iodine cell during the calibration.

Fig. 5 shows the LIF intensity vs. frequency deduced by the results of Fig. 4. Figs. 5(a) and 5(b) were taken during bi-directional injection of the laser at the same position (plasma center). The dashed lines are the Zeeman-split LIF signals, the superimposed Zeeman broadening, due to asymmetric $\pm\sigma$ clusters. Since there is no $\mathbf{E}\times\mathbf{B}$ and diamagnetic drift at the plasma center in the magnetized cylindrical plasma, no Doppler shift should be observed at the plasma center. In Figs. 5(a) and 5(b), the frequency shifts (or wavelength shifts), which mean the Doppler shifts, are $\Delta\nu_{DS} = -27.6$ MHz (or $\Delta\lambda_{DS} = +0.04$ pm) in the forward direction (F) from Fig. 2(b) and $\Delta\nu_{DS} = +20.7$ MHz ($\Delta\lambda_{DS} = -0.03$ pm) in the backward direction (B). The plasma drift velocities (or rotation velocities), $v_{DS} = \lambda_0\Delta\nu_{DS}$ or $v_{DS} = \nu_0\Delta\lambda_{DS}$, are 18 m/s toward the laser (F) and 13 m/s away from the laser (B). These small drift velocities may be due to shift in the finite collection area of the fluorescent light,which is less than 1 mm^2, from the plasma center by less than 1 mm. In addition, the frequency shifts in both cases are all lower than an error of ±0.2 pm or $v_{DS} = \pm 90$ m/s as presented in Fig. 4. This result may be compared to the ion drift velocity of 900 m/s from Keesee *et al* [14].

In the presence of a magnetic field, the LIF signal is given by the sum of all Doppler broadened Zeeman splitting components. In this LIF scheme, the Zeeman splitting is composed of three separate line clusters with eighteen transitions: the six π transitions (one π cluster) and twelve σ transitions (two σ clusters). The resulting function can be written as

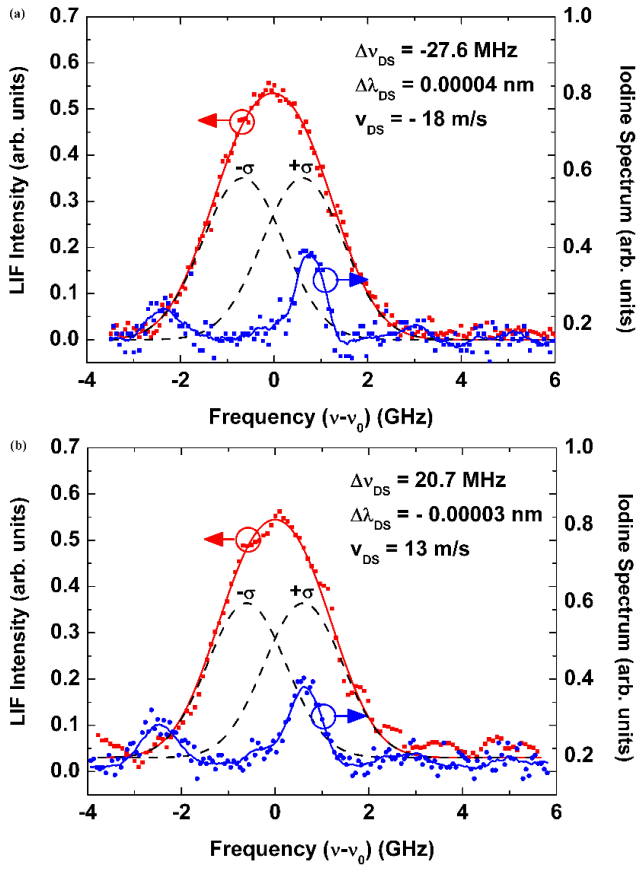

Fig. 5. (Color online) LIF signal and iodine cell spectrum (a) when the laser is injected in the direction of (a) in Fig. 2(b) (from the front side of the chamber to the backside), and (b) when the laser is injected in the direction of (b) in Fig. 2(b) (from the backside to the front side). The dashed lines stand for Zeeman splitting due to asymmetric $\pm\sigma$ clusters imposed Zeeman broadening.

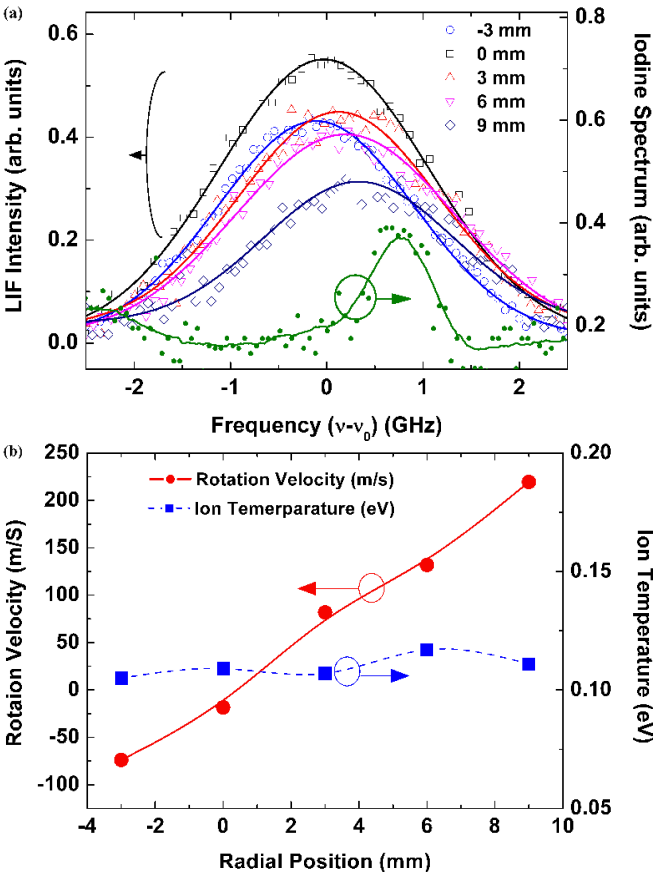

Fig. 6. (Color online) Measurements of the rotational velocity and the ion temperature: (a) LIF intensity and iodine spectrum vs. frequency shift, and (b) the rotational velocity and the ion temperature vs. the radial position.

$$I(\nu) = \sum_{m=0}^{n} I_m(\nu_0 - \Delta\nu_m) \times \exp[\frac{-m_i c^2(\nu - \nu_0 - \Delta\nu_m)^2}{2kT_i\nu_0^2}], \quad (1)$$

where ν_0, k, m_i, c, T_i, n, and $\Delta\nu_m$ are the central frequency (4.4837×10^2 THz or 668.6138 nm) of the Ar ion, the Boltzmann constant, the ion mass, the speed of light, the ion temperature, the number of Zeeman components, and frequency differences caused by the different Zeeman components, respectively [11,26].

When the polarization of the laser is parallel to the magnetic field, only the π components of the Zeeman effects are excited. When the polarization is perpendicular, only the σ components are pumped, as shown in Fig. 5. Boivin and Scime rotated the entire laser by 90° to produce a linear polarization relative to the magnetic field (or only pump the π cluster) when the laser was injected perpendicular to the magnetic field [11]. Since the entire laser was not rotated in this experiment, the measured LIF signals might be superimposed linear polarized components (or Doppler effect) and circularly polarized components (or two asymmetric σ clusters).

The effects of the Zeeman splitting and the Zeeman broadening caused by two asymmetric σ clusters were calculated as $2.22\times10^{-6}B$ nm and $9.0\times10^{-7}B$ nm with B in gauss, respectively [26]. Fig. 6 shows the rotational velocity and the ion temperatures measured by compensating for the Zeeman effects at different radial positions when the lasers were injected in the forward direction (F) in Fig. 2(b). The position of laser injection was moved upward (+) and downward (−) from the center. In the velocity measurement, the (+) sign indicates the Ar ion is moving anti-parallel to the laser while the (−) means it is moving parallel to the laser. Since the laser is injected perpendicular to the magnetic field, this movement is perpendicular to the magnetic field, *i.e.* moving in the azimuthal direction, which indicates that there is an azimuthal plasma rotation. The rotation velocity was increased up to 200 m/s at 9 mm from the center, but remains near 0 m/s at the plasma center, while the ion temperature remains near 0.11 ± 0.005 eV.

IV. SUMMARY

A new LIF system with a single tunable diode laser was developed for the Diversified Plasma Simulator (DiPS). The system has a divertor and space plasma simulators. The accurate measurements of the IVDF, the ion temperature, and the ion drift velocity by LIF strongly depends upon the absolute calibration of the wavelength of the diode laser during the wavelength scan, which is not easily achieved because of the non-linear characteristics of the piezo-electric actuator for the wavelength scan, the narrow mode-hop free tuning range, and the uncertainty of the wavemeter. The wavelengths of the iodine peaks were newly calibrated by using a wavemeter with an absolute calibration and the method of bi-directional injection of the laser, and the results were compared with the previous results obtained by Keesee *et al.* [14], and seemed to agree within 0.002 nm. The new results are different from Keesee *et al.* by 0.002 nm, yet these newly corrected results agree well with the iodine cell spectrum calculated with the Dunham coefficient [24,25]. Because the ion temperature and the drift velocity (or its direction) were not changed while the laser's direction was changed, *i.e.* forward injection and backward injection, the same Doppler effect was observed. Hence, the present result may be more suitable for measuring the ion temperature and its drift velocity than the previous result [14].

ACKNOWLEDGMENTS

This work is supported by the National Research Laboratory Program of the Korea Science and Engineering Foundation (KOSEF) under the Ministry of Science and Technology (MOST) of Korea. The authors thank Prof. G. Severn of University of San Diego for his keen comments on the LIF set-up and data processing, and Prof. Cha-Hwan Oh of Hanyang University for the loan of their wavemeter.

REFERENCES

[1] R. A. Stern and J. A. Johnson, III, Phys. Rev. Lett. **34**, 1548 (1975).
[2] O. Jensen, Contri. Plasma Phys. **42**, 516 (2002).
[3] G. D. Severn, X. Wang, E. Ko and N. Hershkowitz, Phys. Rev. Lett. **90**, 145001 (2003).
[4] L. Oksuz, M. A. Khedr and N. Hershkowitz, Phys. Plasmas **8**, 1729 (2003).
[5] E. E. Scime, P. A. Keiter, M. W. Zintl, R. F. Balkey, J. L. Kline and M. M. Koepke, Plasma Sources Sci. Technol. **7**, 186 (1998).
[6] E. E. Scime, P. A. Keiter, M. M. Balkey, R. F. Boivin, J. L. Kline, M. Blackburn and S. P. Gary, Phys. Plasmas **7**, 2157 (2002).
[7] W. A. Noonan, T. G. Jones and P. F. Ottinger, Rev. Sci. Instrum. **68**, 1032 (1997).
[8] K. Niemi, V. S. von der Gathern and H. F. Dobele, Plasma Sources Sci. Technol. **14**, 315 (2005).
[9] D. A. Edrich, R. McWilliams and N. S. Wolf, Rev. Sci. Instrum. **67**, 2812 (1996).
[10] G. D. Severn, D. A. Edrich and R. McWilliams, Rev. Sci. Instrum. **69**, 10 (1998).
[11] R. F. Boivin and E. E. Scime, Rev. Sci. Instrum. **74**, 4352 (2003).
[12] R. McWilliams and L. Hiderbrandt (private communication).
[13] G. Gersternkorn and P. Luc, *Atlas Du Spectre D'absorption De La Molecule D'iode* (Editions Du Centre National De La Recherche Scientifique, Anatole, 1978), p. 10.
[14] A. M. Keesee, E. E. Scime and R. F. Boivin, Rev. Sci. Instum. **75**, 4091 (2004).
[15] H.-J. Woo, Y.-S. Choi, H.-J. You, S.-Y. Kim, J.-S. Ahn, J.-J. Do, M.-J. Lee and K.-S. Chung, Bull. Am. Phys. Soc. **49**, 128 (2004).
[16] Sacher Lasertechnik, Instruction Manual, Hannah Arendt Str. 3-7, D-350037 Marburg, Germany (2004).
[17] Newport Corporation, 1791 Deere Avenue, (Irvine, CA 92606, USA).
[18] Triad Technology Inc., 1853 Longmont, CO 80502, USA.
[19] Stanford Research Systems, Inc., 1290-D Reamwood Ave., (Sunnyvale, CA 94089, USA).
[20] NTE Electronics, Inc., Bloomfield, NJ 07003, USA.
[21] Andover Coporation, 4 Commercial Drive, (Salem, NH 03079-2800, USA).
[22] Burleigh Instruments, Burleigh Park, P. O. Box E, Fishers, (NY 14453, USA).
[23] JDS Uniphase Corporation, 1768 Automation Parkway, (San Jose, CA 95131, USA).
[24] S. Gerstenkorn and P. Luc, J. Physique. **46**, 867 (1985).
[25] G. D. Severn and C. Sansonetti (private communication).
[26] R. F. Boivin, West Virginia University Plasma Physics Lab. Report PL-50, EPAPS-E-HPAEN-10-003306 (2003).